

advances.sciencemag.org/cgi/content/full/6/3/eaax5145/DC1

Supplementary Materials for **The Euler spiral of rat whiskers**

Eugene L. Starostin, Robyn A. Grant, Gary Dougill, Gert H. M. van der Heijden, Victor G. A. Goss*

*Corresponding author. Email: gossga@lsbu.ac.uk

Published 15 January 2020, *Sci. Adv.* **6**, eaax5145 (2020)
DOI: 10.1126/sciadv.aax5145

This PDF file includes:

Details of Results

Fig. S1. The RSD graphs for the Euler spiral fits.

Fig. S2. Comparison of residual mean square graphs for circular arc (red), Euler spiral (green), and quadratic curvature (blue) fits.

Fig. S3. Distribution of lengths and the curvature coefficients.

Fig. S4. Distribution of lengths L and coefficients B and A across the mystacial pad matrix.

Fig. S5. Violin plots showing distributions of the coefficients B (left) and A (right) relative to individual animals.

Fig. S6. Distribution of 30 average characteristics of shapes for each mystacial follicle.

Fig. S7. Density of whiskers on the universal Euler spiral.

Fig. S8. Configuration of the right half of the whisker sensory shroud (interactive three-dimensional image).

Fig. S9. Configuration of the right half of the whisker sensory shroud (interactive three-dimensional image).

Fig. S10. A schematic of a whisker in a planar approximation.

Supplementary Material

Details of Results

Across the 15 rats the 516 whiskers are distributed as follows

data set	<i>I</i>								<i>II</i>								total
no. of animals	8								7								15
animal #	1	4	5	6	7	8	9	10	11	12	13	16	17	18	19		
no. of whiskers	23	20	25	24	25	22	13	13	47	43	37	56	58	56	54	516	
	165								351								(S1)

and the following matrix represents the distribution over the mystacial pad (Fig. 1, B)

	1	2	3	4	5	6	7
A	17	17	17	20	12		
B	19	18	20	21	15		
C	20	19	20	20	20	14	3
D	20	20	19	20	17	18	11
E		18	18	16	21	15	11

In addition to the Euler spirals, we have approximated the whisker shapes of the data set *I* with circular arcs and curves having quadratic curvature. Comparison of all three accuracies shows that addition of the quadratic term improves approximation much less than the relative gain obtained by allowing for a linear curvature over circular arcs (Fig. S2).

Figures S3–S5 present distributions of the computed lengths and nondimensionalised coefficients *B* and *A* with respect to the animals and to rows and columns of the mystacial pad. Then by using the mean coefficients $\langle B \rangle$ and $\langle A \rangle$, the unit length shapes were computed and rescaled back to their mean lengths (Fig. 5).

Figures

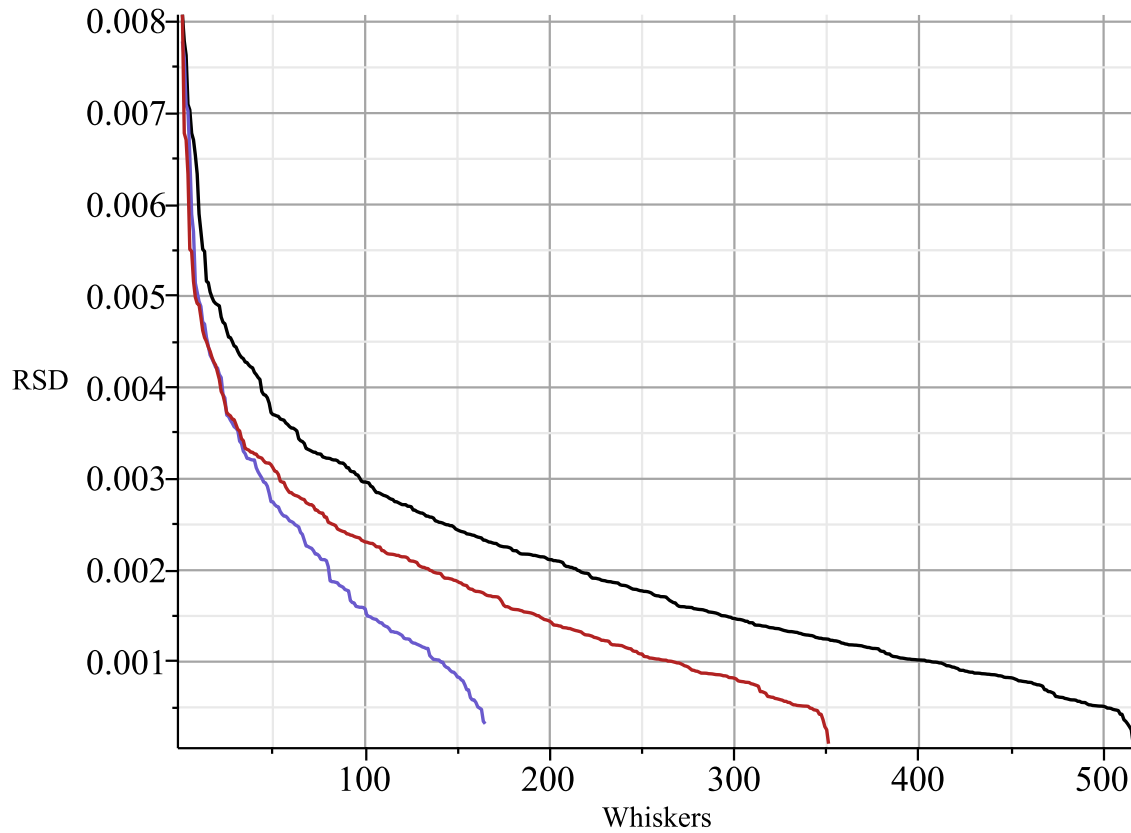


Fig. S1. The RSD graphs for the Euler spiral fits. RSD is calculated as a square root of residual sum of squares $\sum_{i=1}^{N_w} d_i^2$ divided by the number of degrees of freedom, normalised by the length. Data set I (blue), II (red) and their union (black).

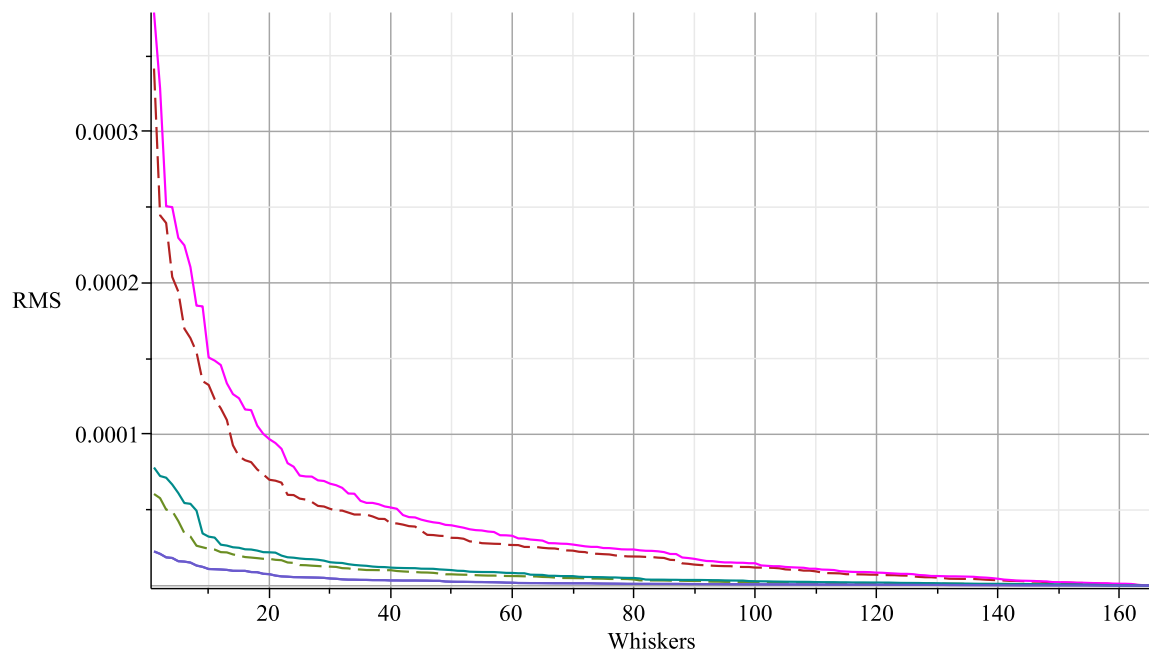


Fig. S2. Comparison of residual mean square graphs for circular arc (red), Euler spiral (green), and quadratic curvature (blue) fits. The solid curves are obtained for 20 grid points and dashed for 100 points, each for a total of 165 rats of data set *I*. RMS is calculated as a residual sum of squares $\sum_{i=1}^{N_w} d_i^2$ divided by the number of degrees of freedom, normalised by the squared length.

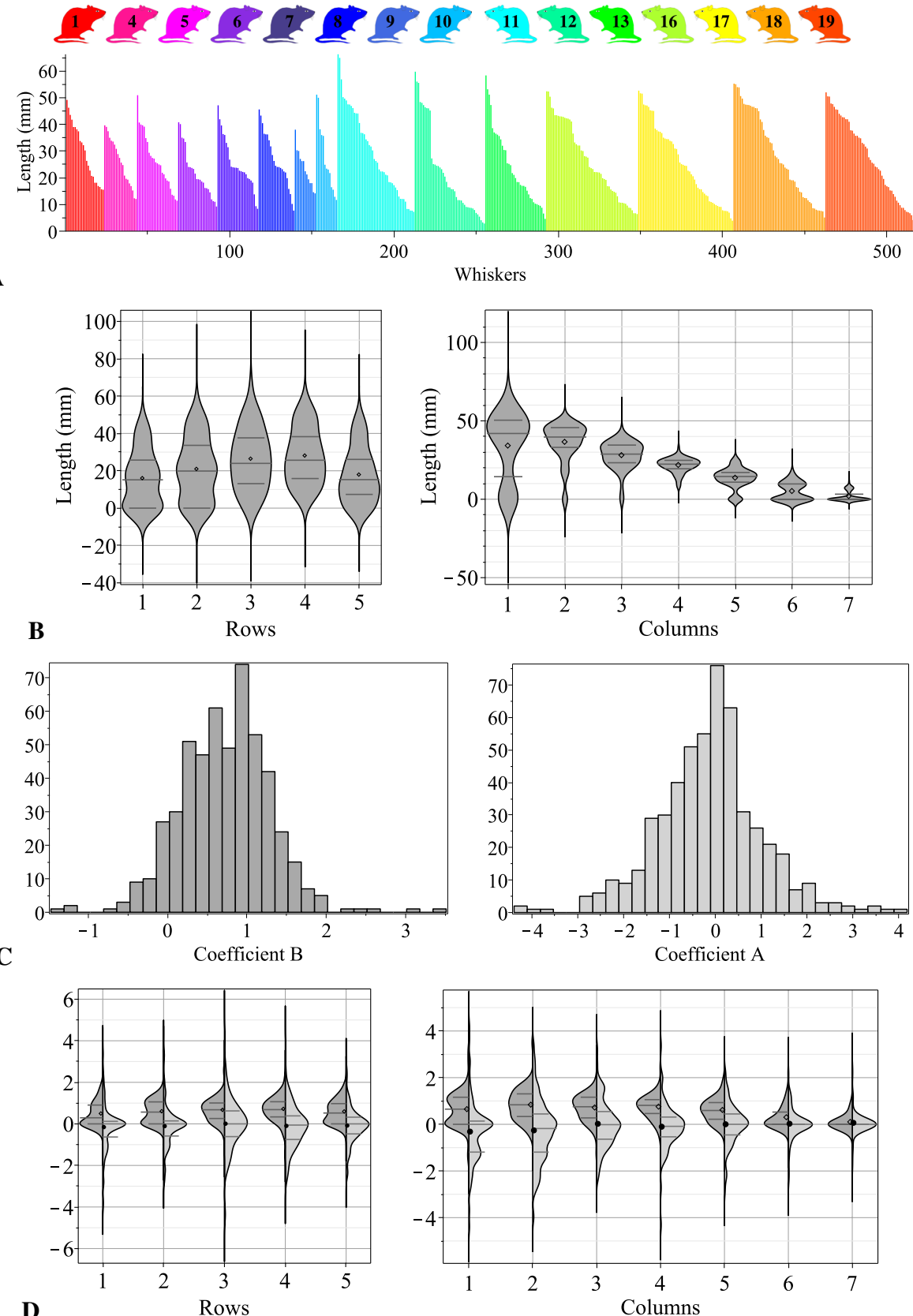


Fig. S3. Distribution of lengths and the curvature coefficients. (A) Ordered whisker lengths for the whole data set. Colours mark individual rats (same as in Fig. 4). The set contains 516 whiskers (see Table S1 for their distribution among animals). (B) Violin plots for distributions of the lengths relative to rows and columns. (C) Histograms of distributions of coefficients B (left) and A (right) for the entire data set. (D) Violin plots for distributions of coefficients B (dark grey left) and A (light grey right) relative to rows and columns. The kernel is set Gaussian in (B, D), the black dots and the horizontal lines mark mean values and quartiles, resp.

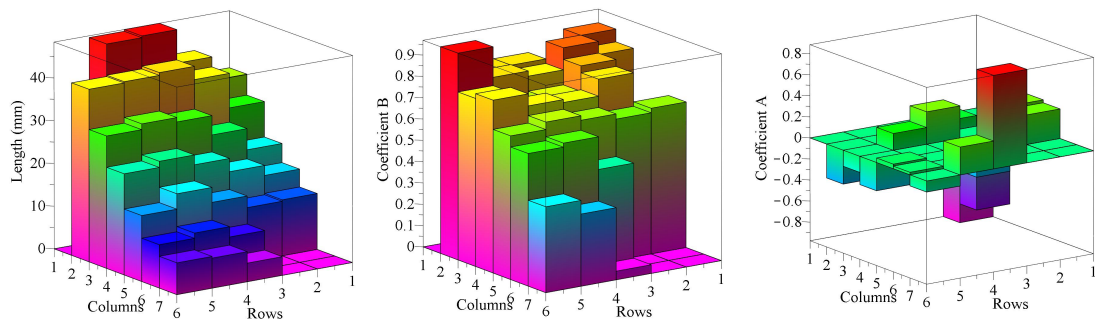


Fig. S4. Distribution of lengths L and coefficients B and A across the mystacial pad matrix.

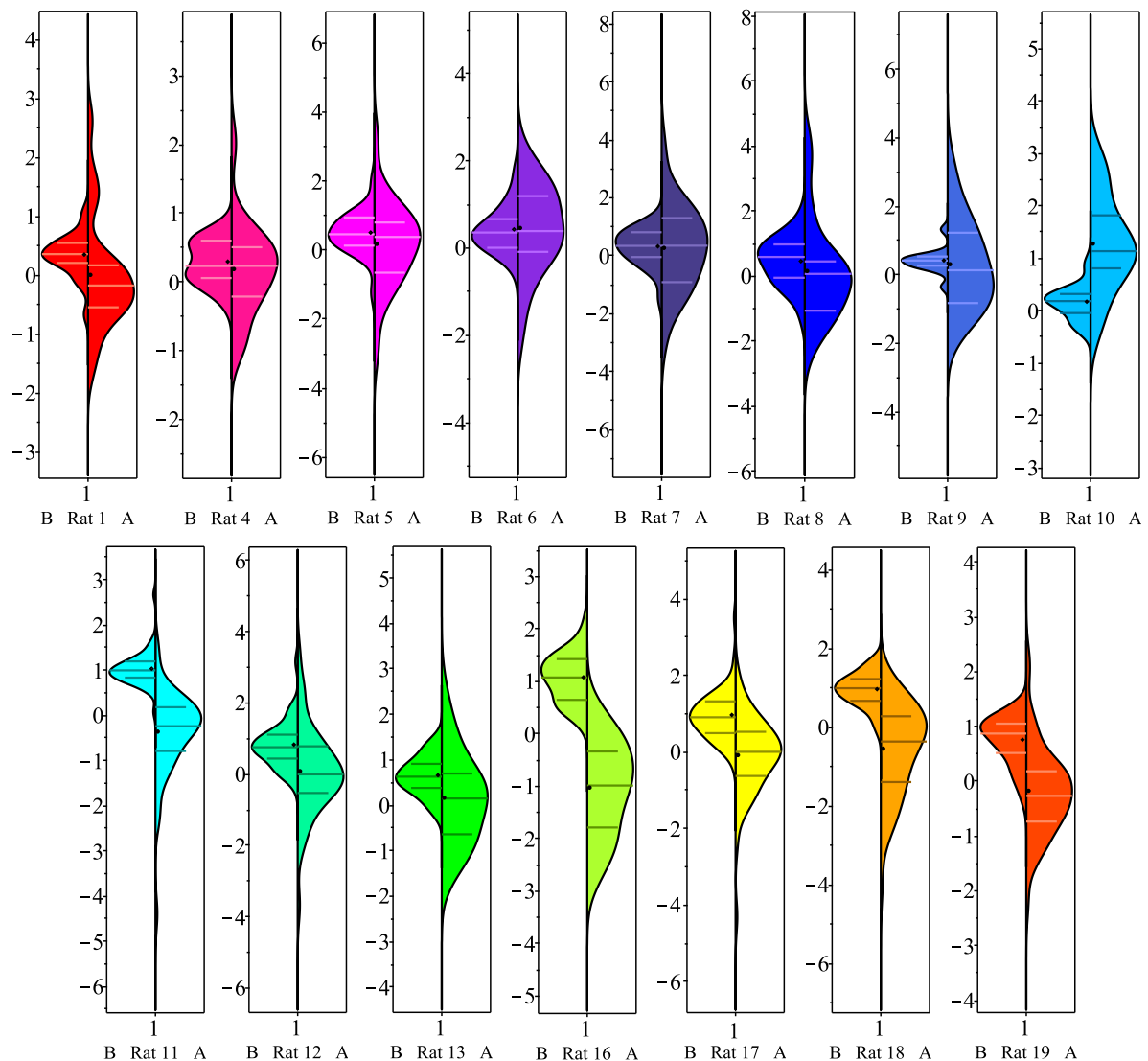


Fig. S5. Violin plots showing distributions of the coefficients B (left) and A (right) relative to individual animals. The kernel is set Gaussian, the black dots and the horizontal lines mark mean values and quartiles, resp. Colours mark 15 different animals (same as in Fig. 4). The upper (lower) row presents the data set I (II), resp.

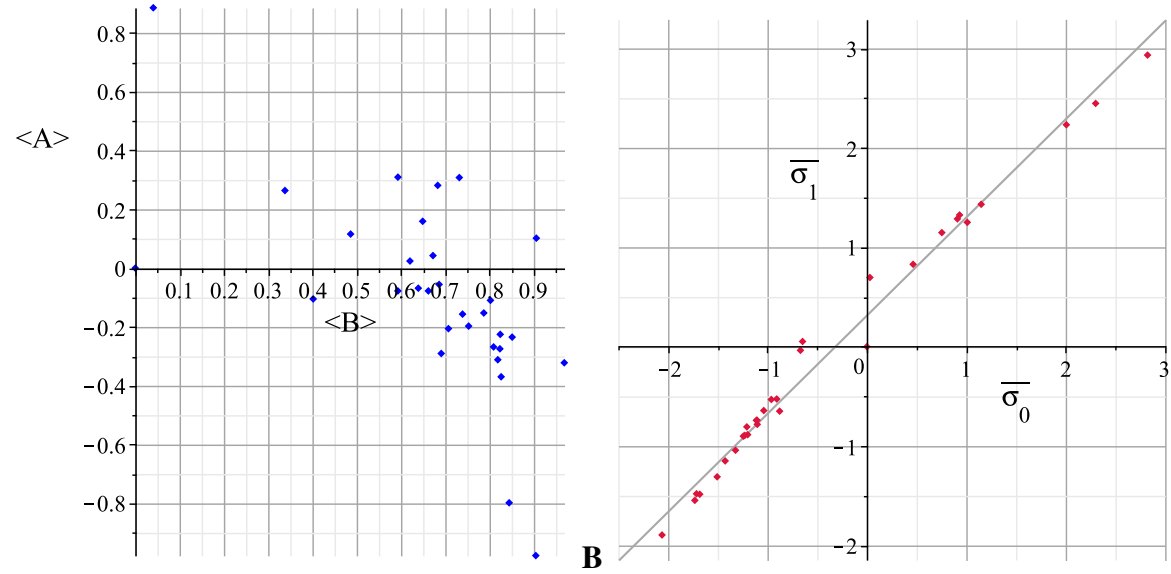


Fig. S6. Distribution of 30 average characteristics of shapes for each mystacial follicle.

(A) Coefficients $\langle B \rangle$ and $\langle A \rangle$. (B) Shape parameters $\bar{\sigma}_0 := \frac{\langle B \rangle}{\sqrt{2}\langle A \rangle}$ and $\bar{\sigma}_1 := \frac{\langle B \rangle}{\sqrt{2}\langle A \rangle} + \sqrt{\frac{\langle A \rangle}{2}}$. The least-squares regression line $\bar{\sigma}_1 = 0.339 + 0.998\bar{\sigma}_0$ with $R^2 = 0.99$.

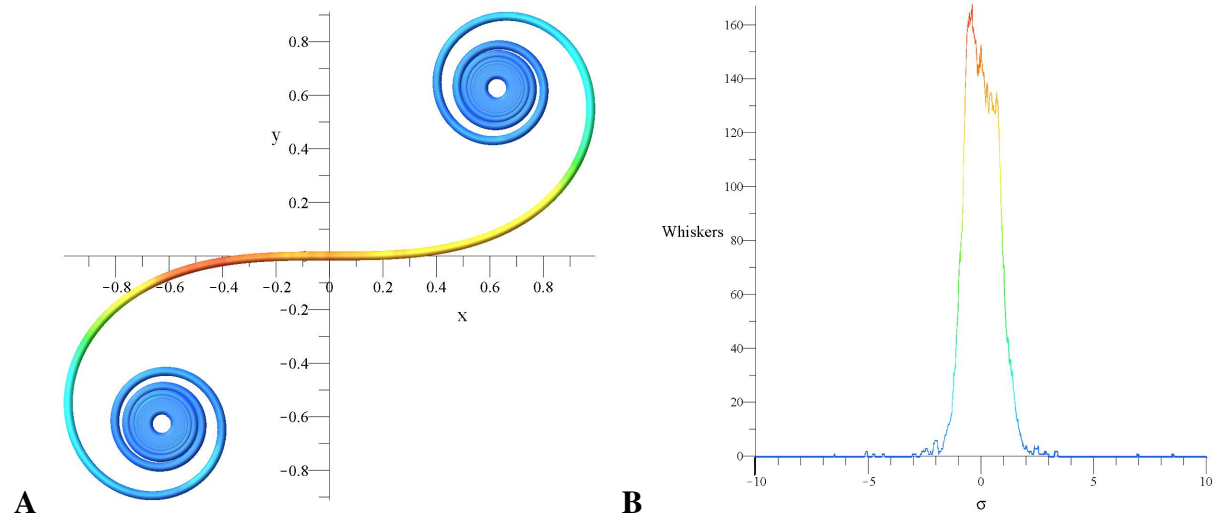


Fig. S7. Density of whiskers on the universal Euler spiral. (A) The Euler spiral coloured according to the number of whiskers mapped to any arc length position. (B) Number of whiskers as a function of the arc length.

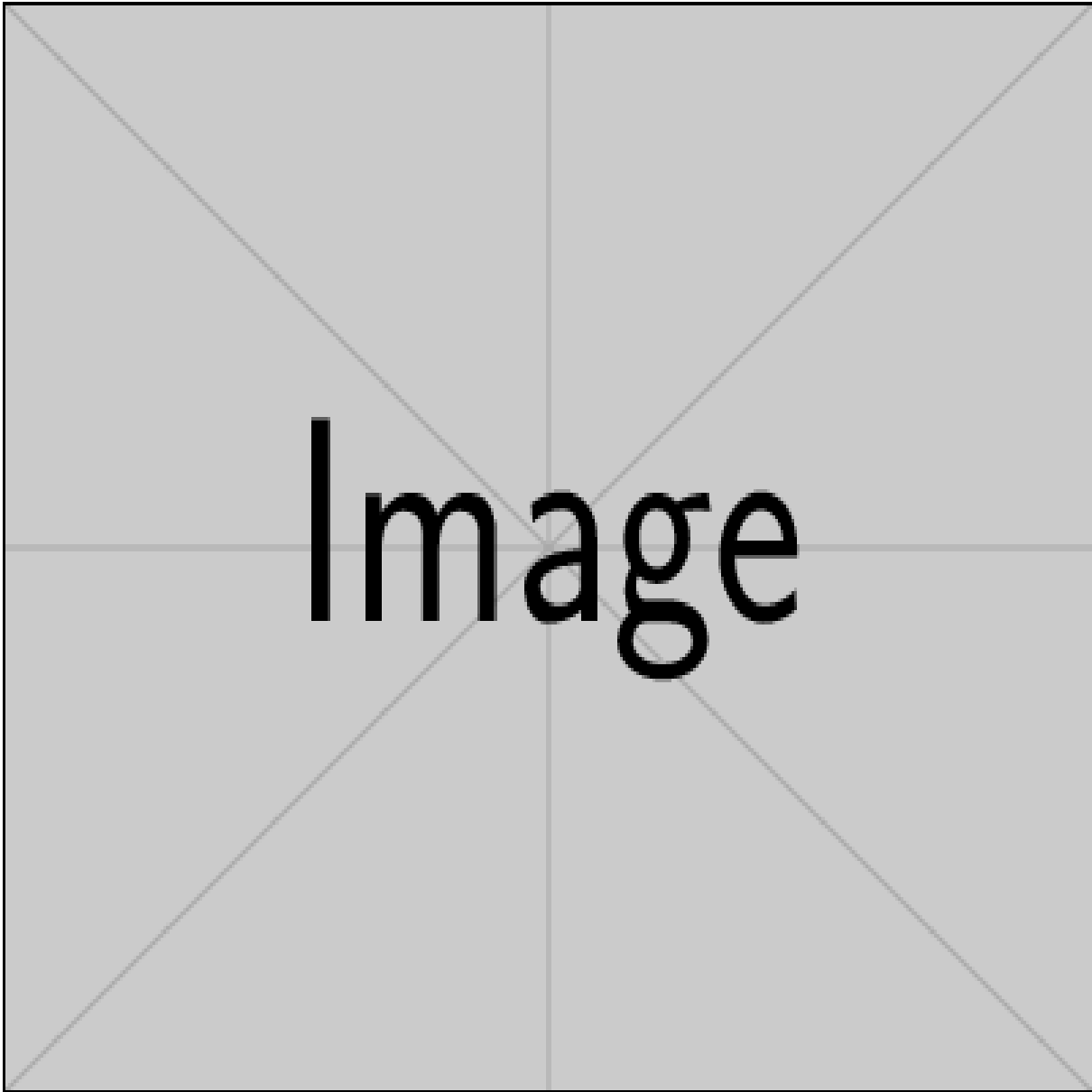


Fig. S8. Configuration of the right half of the whisker sensory shroud (interactive three-dimensional image). The origin $(0,0,0)$ is placed at the mean position of all whisker basepoint locations (for both mystacial pad vibrissae), the xy -plane is the average whisker row plane, the yz -plane is the sagittal plane, the y -axis points rostrally, and the negative y -axis points caudally. Each of the 30 whiskers is represented by an Euler spiral; the blue balls mark the base points at the rat's mystacial pad, the pink balls show the tips. The surface spanned by the whisker tips is shown in yellow.

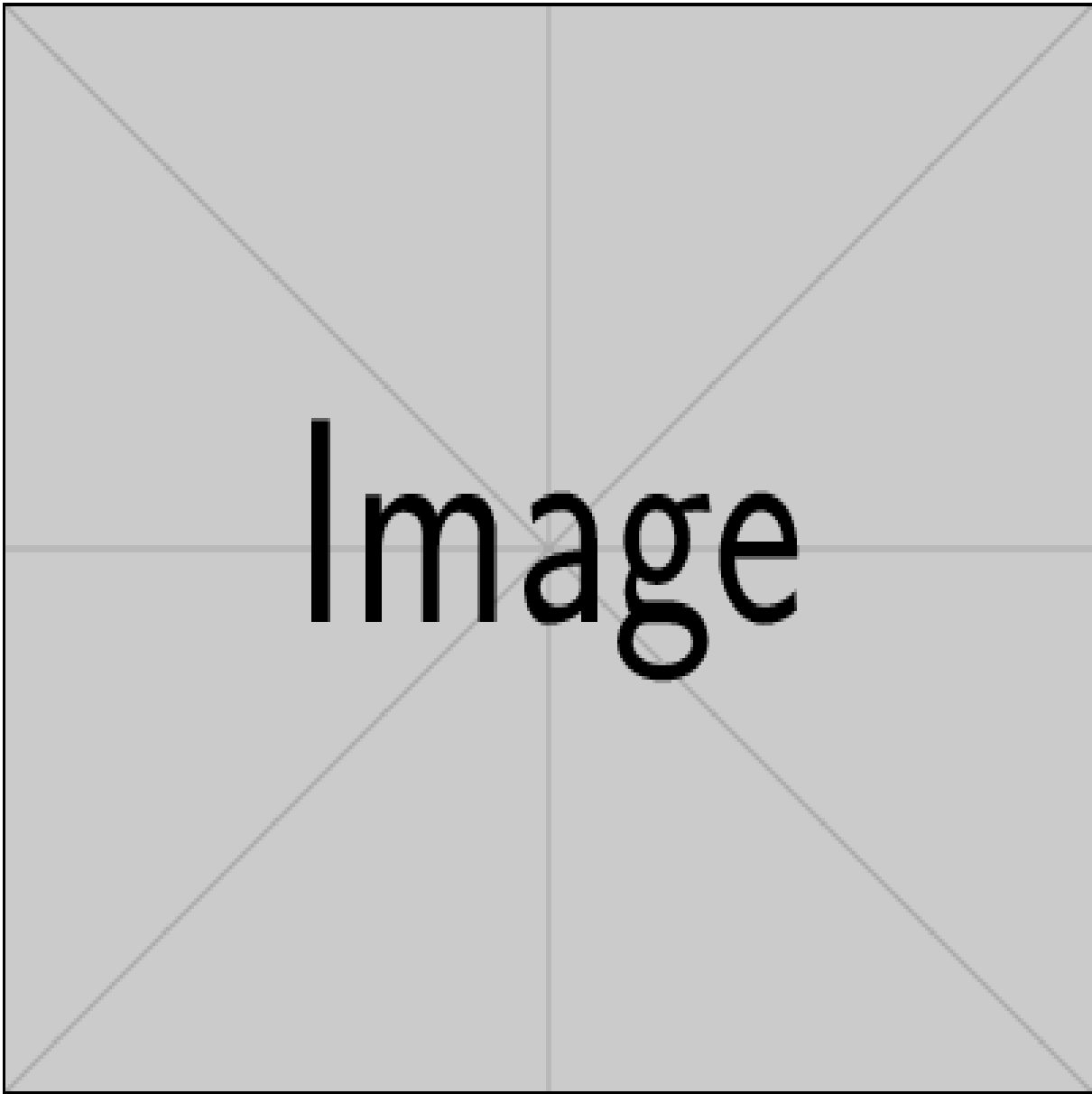


Fig. S9. Configuration of the right half of the whisker sensory shroud (interactive three-dimensional image). The origin (0,0,0) is placed at the mean position of all whisker basepoint locations (for both mystacial pad vibrissae), the xy -plane is the average whisker row plane, the yz -plane is the sagittal plane, the y -axis points rostrally, and the negative y -axis points caudally. Each of the 30 whiskers is represented by an Euler spiral; the blue balls mark the base points at the rat's mystacial pad, the pink balls show the tips. The surface spanned by the whisker tips (yellow) is approximated by an ellipsoid (transparent). Arrows show tangent vectors (light blue) at the tips and normals (red) to the ellipsoidal surface at points closest to the tips; the normals are shifted to the corresponding tips.

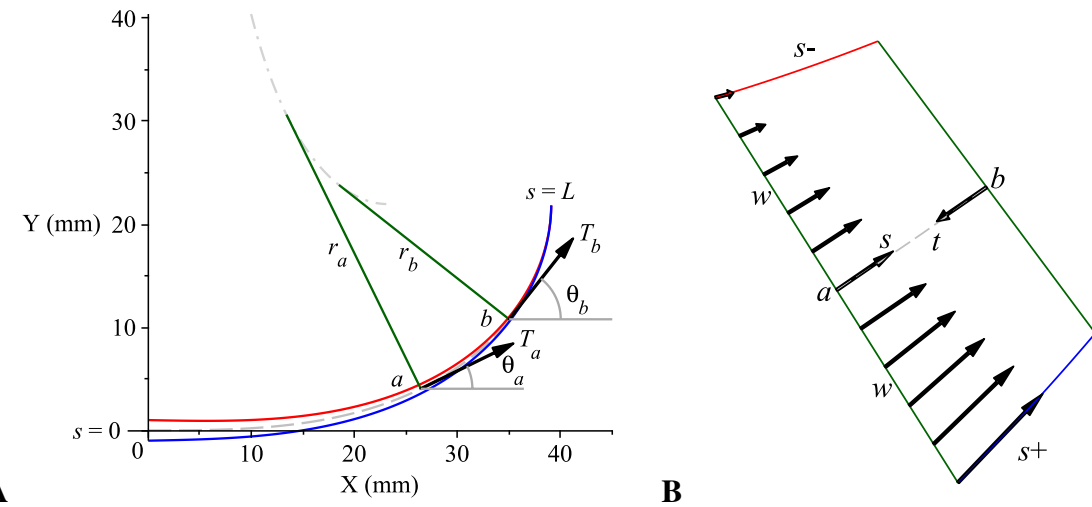


Fig. S10. A schematic of a whisker in a planar approximation. (A) A longitudinal cross-section is shown. The centreline is grey dashed and the two sides are painted red (concave) and blue (convex). The thickness is exaggerated. Green lines show the radii of curvature r_a and r_b in the directions of principal normals to the centreline at two points a and b on the centreline. Their other ends produce an evolute (dash-dotted). The tangent vectors at points a and b , T_a and T_b , make slope angles θ_a and θ_b , resp. (B) A magnified cross-sectional piece $a - b$ of a whisker of width $2w$; s, s^+, s^- are the arc lengths along the centreline (grey dashed), and two sides, resp. An array of arrows indicates the growth rates across section a ; t shows the direction of material accretion with time.